АННОТАЦИЯ к статье

T.I. Gorbunova, A.Ya. Zapevalov, I.V. Beketov, T.M. Demina, O.R. Timoshenkova,A.M. Murzakaev, V.S. Gaviko, A.P. Safronov, V.I. Saloutin Preparation and antifrictional properties of surface modified hybridfluorine-containing silica particles// Applied Surface Science 326 (2015) 19–26
Elsevier, 2015

Модифицированные частицы SiO2 были приготовлены по золь-гель технологии в условиях основного катализа с использованием перфторбутилоксирана и перфторбутилметилтиирана в качестве модификаторов. В условиях кислотного катализа были получены не модифицированные наночастицы SiO2. Химически модифицированные наноразмерные частицы SiO2 были охарактеризованы методами ИК-фурье спектроскопии, низкотемпературной сорбции (БЭТ), РФА и энергодисперсионного анализа. Были измерены коэффициенты трения стальных поверхностей при нагрузках 10, 20, 30, 60 Н с использованием масла с добавками 5, 10 , 15% модифицированных частиц SiO2. Наибольшее уменьшение вязкости было зарегистрировано при использовании масла с наиболее низким содержанием добавки. Вероятным механизмом антифрикционного действия является образование граничных смазывающих слоев, содержащих соли железа.

Applied Surface Science 326 (2015) 19–26

Contents lists available at ScienceDirect

Applied Surface Science

journal homepage: www.elsevier.com/locate/apsusc

Preparation and antifrictional properties of surface modified hybrid fluorine-containing silica particles

T.I. Gorbunova[a,*], A.Ya. Zapevalov[a], I.V. Beketov[b], T.M. Demina[b], O.R. Timoshenkova[b], A.M. Murzakaev[b,d], V.S. Gaviko[c], A.P. Safronov[b,d], V.I. Saloutin[a]

[a] I.Ya. Postovskii Institute of Organic Synthesis, Ural Branch, Russian Academy of Sciences, Kovalevskoy Street, 22, Ekaterinburg 620990, Russia
[b] Institute of Electrophysics, Ural Branch, Russian Academy of Sciences, Amundsena Street, 106, Ekaterinburg 620016, Russia
[c] Institute of Metal Physics, Ural Branch, Russian Academy of Sciences, Kovalevskoy Street, 18, Ekaterinburg 620990, Russia
[d] Ural Federal University named after the first President of Russia B.N. Yeltsin, Mira Street, 19, Ekaterinburg 620002, Russia

ARTICLE INFO

Article history:
Received 1 April 2014
Received in revised form
13 November 2014
Accepted 18 November 2014
Available online 24 November 2014

Keywords:
Sol–gel preparation
Surface modification
Covalent bonding
Fluorine-containing oxirane/thiirane
Antifrictional properties

ABSTRACT

Modified SiO_2 particles were successfully prepared via [(perfluorobutyl)methyl]oxirane and [(perfluorobutyl)methyl]thiirane in sol–gel conditions using basic catalysis. As a result of acid catalysis non-modified nano-sized SiO_2 particles were formed. Chemically modified SiO_2 particles were characterized by means of FT-IR, BET, TEM, XRD- and XPS-analyses. Friction coefficients were determined at steel surface for base oil with modified SiO_2 additives (5, 10 and 15 wt.%) at 10, 20, 30 and 60 N loads. Friction was reduced most strongly in the oil mix with the lowest content of the additive. A possible mechanism of antifrictional improvement is the formation of boundary lubrication layers containing iron salts.
© 2014 Elsevier B.V. All rights reserved.

1. Introduction

At present, there can be distinguished three main methods to modify the surface of SiO_2 particles. The first represents occlusion of an organic molecule in a SiO_2 matrix formed at a sol–gel process using tetraalkoxysilanes [1]. In this case, on the surface of the inorganic phase the SiO_2 particles are modified due to physical adsorption of organic molecules in the reaction zone. Useful materials thus obtained do not find application in solutions since the organic phase is rapidly washed away from the SiO_2 surface.

Methods from the second group are the most developed. These are based on a sol–gel process in the presence of tetraalkoxysilane and silane containing substituents that are not prone to hydrolysis [2]. It is these substituents that modify the surface of SiO_2 particles. Materials thus synthesized were named ormosil. They serve as the basis for sensors for biomolecules [2], lubricants [3], anticorrosive coatings [4], etc.

The smallest is the third group of methods. Their goal is to develop covalent bonding between SiO_2 particles and organic molecules not containing silicon atoms. As a rule, the implementation of such processes makes use of commercial SiO_2 particles. At first they are activated with the surface free HO groups actively formed (SiO_2—OH). Then the interactions between SiO_2—OH and reactive organic molecules come into play. The technique is named "grafting technology" and used widely for encapsulation of SiO_2 particles in organic polymeric matrixes [5–7].

Interaction of silanol group Si—OH formed in situ as a result of tetraalkoxysilane hydrolysis at the first stage of sol–gel process with reactive organic molecules containing no silicon atoms belongs to the same group of modification methods. The free silanol group has two lone electron pairs at the oxygen atom and is mild nucleophile [8]. When the Si—OH group interacts with the organic substrate a new covalent bond Si—O—Y is formed (where Y is part of the organic molecule). The polymeric SiO_2 grid formed at the second stage of sol–gel synthesis is modified by organic substituents partially. The success of the process depends on favorable reactive conditions and the organic precursor.

Oxirane and thiirane rings are reactive groups in organic chemistry. These functional units are capable of regioselective ring-opening via nucleophilic reagents [9,10]. In the present work, we studied (i) surface modification of SiO_2 particles formed in situ via fluorine-containing oxirane and thiirane and (ii) antifrictional properties of modified SiO_2 particles as additives to oil.

* Corresponding author. Tel.: +7 343 369 3058; fax: +7 343 369 3058.
E-mail address: gorbunova@ios.uran.ru (T.I. Gorbunova).

http://dx.doi.org/10.1016/j.apsusc.2014.11.091
0169-4332/© 2014 Elsevier B.V. All rights reserved.

2. Experimental

2.1. Materials

Tetraethoxysilane (TEOS) (98%, Aldrich), hydrochloric acid HCl (cp grade, Russia), triethyl amine NEt_3 (cp grade, Russia) were used. [(Perfluorobutyl)methyl]oxirane (bp 144–146 °C) and [(perfluorobutyl)methyl]thiirane (bp 144–147 °C) were prepared as described earlier in Refs. [11,10], respectively.

2.2. Synthesis of modified SiO_2 particles

Typically, at room temperature a 25 ml round-bottom flask equipped with a magnetic stirrer and reflux condenser was charged with 0.01 mol TEOS, 0.06 mol H_2O, 0.011 mol [(perfluorobutyl)methyl]oxirane (or [(perfluorobutyl)methyl]thiirane) and 50 μl HCl (or NEt_3). The mixture was heated to boiling and kept so for 2 h. Compounds having a low boiling point were distilled off to 150 °C. White powders were obtained.

2.3. Sample characterization

Infrared spectra (4000–400 cm^{-1}) were recorded using an FT-IR spectrophotometer (Perkin Elmer, SPECTRUM ONE).

The BET specific surface area was determined from the low temperature absorption of nitrogen with a Micromeritics TriStar 3000. In order to eliminate the volatile components, the isothermal measurements were made after evacuating the sample space continuously for 1 h at 100 °C.

The morphology and size of the powder samples were analyzed using JEM 2100 (JEOL, Hitachi) transmission electron microscope (TEM). The samples were first dispersed in *i*-propanol at 20 kHz and 0.5 kV. Then 50 μl of the resulting suspension were deposited on a copper grid with diameter of 3 mm and dried in the closed Petri's cups at ambient conditions.

The crystal structure was characterized by X-ray power diffraction (XRD) using DRON-6 automatic diffractometer in a Cr Kα radiation.

X-ray photoelectron spectroscopy (XPS) was performed using a VG ESCALAB MK II electron spectrometer. The vacuum in the analyzer chamber of the spectrometer during the measurements was maintained at 10^{-8} Pa, and an Mg Kα radiation (1256.3 eV) was used as the excitation radiation. The energy scan step was 0.1 eV, the spectrometer calibration was performed over the Au 4*f*7/2 line (84 eV), and the sample charge was estimated on the carbon spectra C 1*s* (284.5 eV) from the natural hydrocarbon contaminations on the surface. The measurements were made at the angle $\Theta = 90°$ between the sample surface and the analyzer axis. The maximum depth of the XPS analysis was achieved at approximately 3–4 nm from the surface layer.

2.4. Tribology tests

The friction coefficient of the base oil (a viscosity class 32 (DIN 51 516, ISO 3448-75)) with modified SiO_2 particles was measured using a tribometer (CSM Instruments) with a ball-on-disk configuration. Balls (diameter 10 mm) and disks (diameter 35 mm) are made of GCr15 bearing steel (C, 0.95–1.05 wt.%; Si, 0.15–0.35 wt.%; Mn, 0.20–0.40 wt.%; P, 0.027 wt.%; S, 0.020 wt.%; Cr, 1.30–1.65 wt.%; Ni, 0.30 wt.%; Cu, 0.25 wt.%) with an initial Rockwell hardness (in C scale) 60–63. Friction tests were performed at a rotation speed of 8 cm s^{-1}, a load (10, 20, 30 and 60 N) and for a duration of 10,000 cycles. The oil dose for each measurement was 100 μl. Every test was repeated five times to reach an accuracy of 0.001–0.002.

3. Results and discussion

3.1. Reaction mechanism

The surface modification of SiO_2 particles was carried out at sol–gel process using TEOS and acidic (HCl) or basic (NEt_3) catalysis (Scheme). As usual, the first step is the TEOS hydrolysis [8]. The second step is an attack of the silanol group on the end carbon atom of [(perfluorobutyl)methyl]oxirane or -thiirane. It leads to a regioselective opening of the oxirane (thiirane) ring and to the formation of an unstable intermediate **A1**. The third step is the stabilization of **A1** by means of hydrogen transfer and the formation of **A2**.

As a result, four products were obtained: $\mathbf{SiO_2\text{-}A_O}$ and $\mathbf{SiO_2\text{-}A_S}$ by acidic catalysis with [(perfluorobutyl)methyl]oxirane and -thiirane, respectively, $\mathbf{SiO_2\text{-}B_O}$ and $\mathbf{SiO_2\text{-}B_S}$ by basic catalysis with [(perfluorobutyl)methyl]oxirane and -thiirane, respectively. In order to compare the analytic parameters of the samples, a **SiO_2-matrix** was synthesized in the same conditions by acidic catalysis without fluorine-containing compounds.

3.2. FT-IR study

The FT-IR spectrum of the **SiO_2-matrix** is classic (Fig. 1a) and corresponds to numerous data from literature, e.g., those in Refs. [12–14]. The FT-IR spectrum of the [(perfluorobutyl)methyl]oxirane (Fig. 1b) exhibits the characteristic strong absorption bands of the C—O—C groups at 1133 cm^{-1} and of the C—F groups at 1223 cm^{-1} and weak bands of the C—H groups at 2934, 3011 and 3062 cm^{-1}. The FT-IR spectra of the [(perfluorobutyl)methyl]oxirane and -thiirane are similar for the absorption region of the C—F groups. Fig. 1c shows the FT-IR spectrum of $\mathbf{SiO_2\text{-}A_O}$. It displays the weak bands of the C—O—C (1132 cm^{-1}) and the C—F (1220 cm^{-1}) groups, while C—H absorption bands are absent. On the contrary, the strong bands of the C—O—C (1132 cm^{-1}) and the C—F (1221 cm^{-1}) groups are observed in the FT-IR spectrum of $\mathbf{SiO_2\text{-}B_O}$ (Fig. 1d). Additionally, a weak band of the C—H groups appears at 2984 cm^{-1}. It should be noted that in the FT-IR spectrum of $\mathbf{SiO_2\text{-}A_O}$ the intensity of the O—H bands at 3405 cm^{-1} decreases in comparison with those at 3372 cm^{-1} for $\mathbf{SiO_2\text{-}B_O}$. This confirms that the $\mathbf{SiO_2\text{-}A_O}$ sample is more surface hydrophobic than $\mathbf{SiO_2\text{-}B_O}$ [14]. The FT-IR spectra of $\mathbf{SiO_2\text{-}A_S}$ and $\mathbf{SiO_2\text{-}B_S}$ are similar to those of $\mathbf{SiO_2\text{-}A_O}$ and $\mathbf{SiO_2\text{-}B_O}$, respectively.

3.3. Surface area measurements and study of surface morphology

Measurements of specific surface area by the BET method yielded the following values: 279.752 $m^2 g^{-1}$ for $\mathbf{SiO_2\text{-}A_O}$, 328,465 $m^2 g^{-1}$ for $\mathbf{SiO_2\text{-}A_S}$, 1.944 $m^2 g^{-1}$ for $\mathbf{SiO_2\text{-}B_O}$ and 5.541 $m^2 g^{-1}$ for $\mathbf{SiO_2\text{-}B_S}$. It should be noted that the $\mathbf{SiO_2\text{-}A_O}$ and the $\mathbf{SiO_2\text{-}A_S}$ samples strongly emitted gas during preparation for the measurements and their volume decreased appreciably. It confirms indirectly the absence of covalent bonding of the [(perfluorobutyl)methyl]oxirane and -thiirane with the SiO_2 surface in $\mathbf{SiO_2\text{-}A_O}$ and $\mathbf{SiO_2\text{-}A_S}$. It is possible that in this case the organic molecules were bonded with the inorganic matrix owing to physical adsorption and removed from the SiO_2 surface in vacuum. The $\mathbf{SiO_2\text{-}B_O}$ and $\mathbf{SiO_2\text{-}B_S}$ samples were stable during preparation for the BET method.

The $\mathbf{SiO_2\text{-}A_O}$ and $\mathbf{SiO_2\text{-}A_S}$ samples consist of nano-sized particles, which is confirmed by TEM (Fig. 2a and b). Both samples are amorphous and agglomerated but contain individual faceted particles with a size of 30–80 nm. These particles are probably crystalline. Primary particles of $\mathbf{SiO_2\text{-}A_O}$ (Fig. 2a) have average particle size of about 15 nm. The particle size of $\mathbf{SiO_2\text{-}A_S}$ (Fig. 2b) is 3–5 nm.

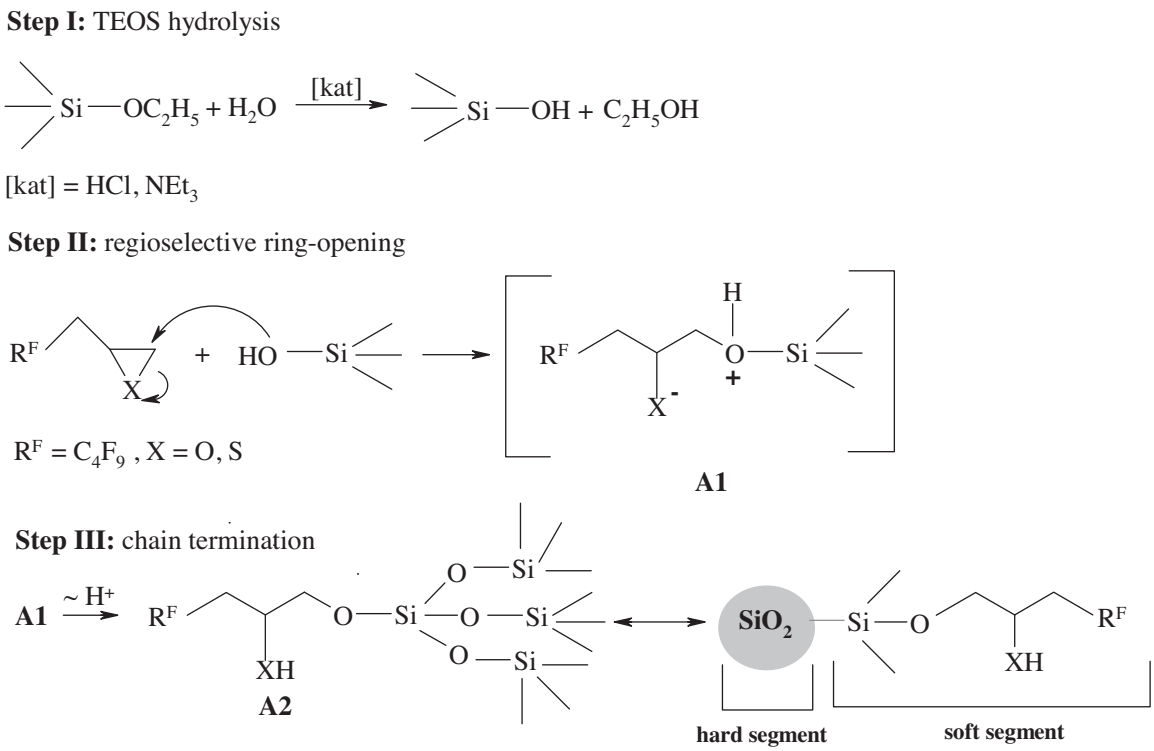

Scheme 1. Three-step route for the surface modification of SiO_2 particles via [(perfluorobutyl)methyl]oxirane or [(perfluorobutyl)methyl]thiirane.

3.4. XRD analysis

The diffraction profiles for **SiO_2-A_O**, **SiO_2-B_O** and **SiO_2-B_S** are similar. They represent peaks of amorphous haloes with the following values of 2θ: 34.4°, 35.6° and 34.8° for **SiO_2-A_O**, **SiO_2-B_O** and **SiO_2-B_S**, respectively. A typical X-ray diffraction pattern is shown in Fig. 3. All registered diffraction profiles are similar to the amorphous haloes obtained for high-purity commercial amorphous quartz in a Cu Kα radiation (2θ = 22.5°) [15]. Generally the XRD analysis does not give precise information about the type of bonding between organic molecules and SiO_2 particles, in contrast to an XPS study.

3.5. XPS study

During XPS analysis the **SiO_2-A_O** and **SiO_2-A_S** samples strongly emitted gas. The vacuum in the analyzer chamber of the spectrometer deteriorated. For this reason, XPS allowed us to determine only the presence of silicon and oxygen atoms in the **SiO_2-A_O** and the **SiO_2-A_S** samples.

XPS results for **SiO_2-B_O** and **SiO_2-B_S** estimate atomic concentration as listed in Table 1. Atomic ratios [O]:[Si] determined for **SiO_2-B_O** and **SiO_2-B_S** are 1.23 and 1.66, respectively. These values do not correspond to non-modified SiO_2 particles. In Ref. [16] a crystal and three amorphous samples of SiO_2 were investigated. The atomic ratio [O]:[Si] for all samples was found to lie in the range 2.50–2.70.

Table 1
Atomic percentages of C, Si, O, F and ratios [O]:[Si] of the **SO_2-B_O** and the **SO_2-B_S** samples.

Sample	C (%)	Si (%)	F (%)	O (%)	[O]:[Si]
SO_2-B_O	22.5	21.5	23.9	26.5	1.23
SO_2-B_S[a]	28.0	14.3	31.2	23.8	1.66

[a] Atomic percentages of S are 2.3%.

The XPS Si 2p spectra of **SiO_2-B_O** and **SiO_2-B_S** are presented as a doublet of Si $2p_{3/2}$ and Si $2p_{1/2}$ peaks not resolved energetically (Fig. 4a). The binding energy value in both cases is similar to that for non-modified SiO_2 particles in Ref. [16] and for modified SiO_2 particles in Ref. [17]. It is reasonable to assume that there are two spectrally close chemical modifications of Si.

In the XPS C 1s spectrum of **SiO_2-B_O** a number of non-equivalent states are found (Fig. 4b). The two peaks at high binding energy are related to CF_2 and CF_3 bonds [17]. The peaks at low binding energy belong to CH_2 bonds [18,19]. The two peaks in the center including the most intensive are resolved less accurately. They might be related to carbon–hydrogen and carbon–oxygen bonds [18,19]. The XPS C 1s spectrum of **SiO_2-B_S** is similar (Fig. 4b).

The XPS O 1s spectra of **SiO_2-B_O** and **SiO_2-B_S** indicate that oxygen is in a single state (Fig. 4c) [20]. The O 1s signals represent broad peaks. It is known that broad O 1s peaks can be due to a superposition of several spectrally close signals which cannot be resolved [21]. For instance, in Refs. [22,23] the XPS O 1s spectra are presented both for modifying reagents and for modified SiO_2 particles. For the XPS O 1s spectrum for cetyltrimethyloxysilane there are two peaks for O—Si and O—C at 533.2 and 535.2 eV, respectively [22]. After modifying the SiO_2 particles by means of cetyltrimethyloxysilane the XPS O 1s spectrum of the organic–inorganic material represents a single broad peak at 532.0 eV.

The same result is reported in Ref. [23], where the XPS O 1s spectrum for polyimide is represented by a doublet for the C=O and C—O—C groups at 531.9 and 533.2 eV, respectively. But for the hybrid SiO_2/polyimide particles the XPS O 1s peak was a singlet at 532.5 eV combining all possible oxygen states with other atoms. The authors of Ref. [23] claim that the O 1s binding energy shift at 532.5 eV is associated with the Si—O—Si vibrations and the functional groups of the polyimide cannot be identified. In Refs. [24,25] XPS O 1s spectra for SiO_2/polyacrylate and SiO_2/poly(γ-(carbamic acid benzyl ester)-ε-caprolactone) samples are presented as well. These hybrid materials have O=C—O, C—O, Si—O [24] and O=C—O,

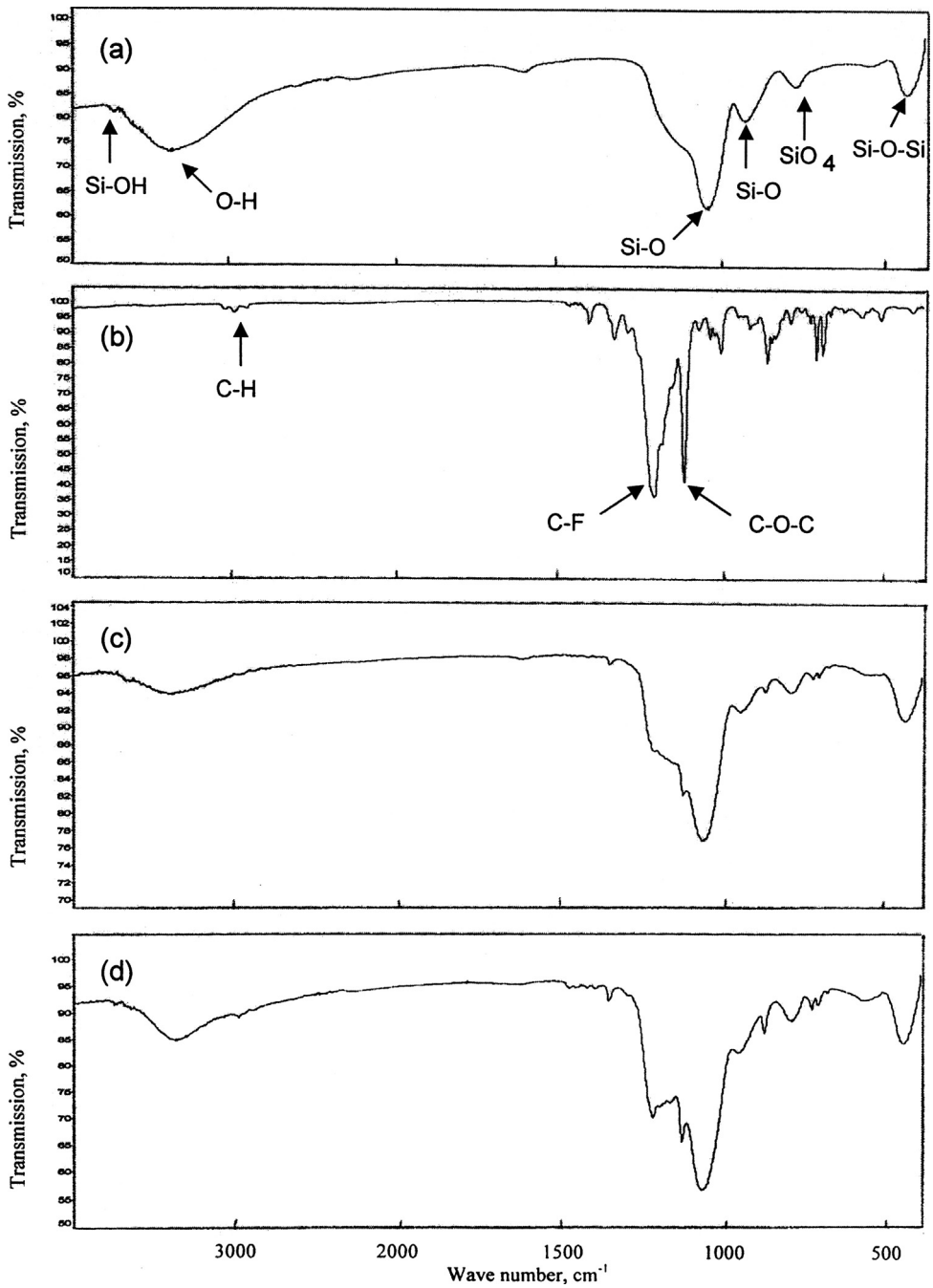

Fig. 1. FT-IR spectra of the **SiO_2-matrix** (a), [(perfluorobutyl)methyl]oxirane (b), **SiO_2-A_O** (c) and **SiO_2-B_O** (d).

H—O, Si—O [25], respectively, but the XPS O 1s spectrum is a singlet in both cases.

At the same time there are examples where XPS O 1s spectrum can be resolved successfully. In Refs. [26–28] the O=C—O and C—O states in the O 1s binding energy shifts are visualized. For polymers containing OH, C—O—C, O=C—O and O=C groups the XPS O 1s spectra are more complicated [29]. Signals can be present in pairs in the same area as OH and C—O—C at 532.8 eV or as O=C—O and O=C at 532.2 eV. Interaction between hard and soft segments of the synthesized organic–inorganic particles is the main reason for the various manifestations of O 1s signals [30] (see Scheme).

For the synthesized the **SiO_2-B_O** and the **SiO_2-B_S** samples the formation of intra- and intermolecular hydrogen bonds of HO. . .H, HS. . .H and H. . .F types may be the most probable [31–35]. HO groups can be found both on the surface of SiO_2 particles and on part of the soft segment at **SiO_2-B_O** and **SiO_2-B_S**. Obviously, not only spectrally close signals of the functional HO, Si—O—C, Si—O—Si groups influence the XPS O 1s peak but the hydrogen bonds formed onto the SiO_2 surface do as well.

In spite of the broad XPS signal for the F 1s, it reflects a single state in the **SiO_2-B_O** and **SiO_2-B_S** samples (Fig. 4d). Fluorine states from individual bonds in CF_2 and CF_3 groups are not visible, in contrast to carbon C 1s. In the literature there are many data on XPS for F 1s registered for the CF_3-, CF_2- and CF-groups in the same product. As a rule, the XPS peak for F 1s represents an unresolved signal and various conditions of F 1s cannot be visualized independently of the X-ray source (Mg Kα- or Al Kα-radiation). It is characteristic for fluorinated polymers [36–40], polymers grafted onto various solid films [41–44] and SiO_2 particles [45–47]. For the presented cases the binding energy of strong F 1s at XPS spectra is

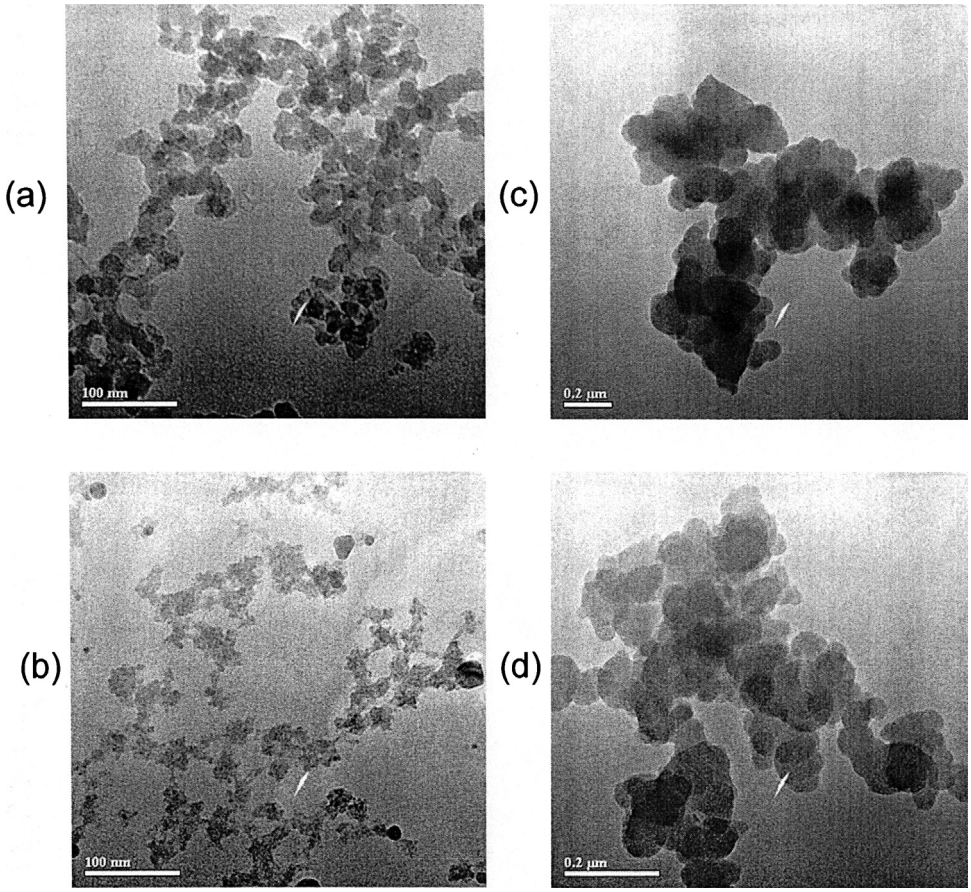

Fig. 2. TEM images of **SiO_2-A_O** (a), of **SiO_2-A_S** (b), of **SiO_2-B_O** (c) and **SiO_2-B_S** (d).

in the range 687.0–689.1 eV. Possible reasons for these phenomena are flexibility and vibrations of long-chain fluoroalkyl substituents placed onto the surface of SiO_2 particles and oriented away from them [48–51] and the low content of fluorine-containing fragments on the SiO_2 surface when the F 1s signals are shielded by those of the SiO_2 particles from internal volume.

The XPS S 2p spectrum for the **SiO_2-B_S** sample is presented in Fig. 4e. The position of the S 2p peak at 164.0 eV is in close proximity to the Si 2s line. At present it is not possible to determine unambiguously whether the sulfur atom is in the exo- or endocyclic arrangement. However, according to the NIST Standard Reference Database 20 (version 4.1), the binding energy for S 2p corresponds to S—C or/and S—H but not to S—Si or S—O bonds. Besides, there is the S 2s line in the XPS spectrum of **SiO_2-B_S** (Fig. 5). This signal is not superimposed with other peaks and indicates sulfur present in the sample.

Thus, the results of our XPS study show that all necessary elements are present in the structures of **SiO_2-B_O** and **SiO_2-B_S**. The XPS analysis was performed under deep vacuum (10^{-8} Pa). The boiling points of [(perfluorobutyl)methyl]oxirane and -thiirane are low (see Section 2.1) and during the XPS analysis fluorine-containing compounds could be removed from the SiO_2 surface given adhesive bonding. Consequently, the SiO_2 particles in the **SiO_2-B_O** and the **SiO_2-B_S** samples are connected with the fluorine-containing compounds by means of chemical bonding rather than by adhesion.

To summarize, one may assume that the **SiO_2-B_O** and the **SiO_2-B_S** samples represent amorphous SiO_2 having its surface partially modified by means of [(perfluorobutyl)methyl]oxirane and -thiirane.

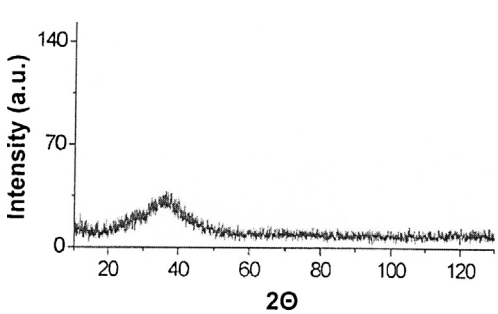

Fig. 3. XRD pattern of the **SiO_2-B_O** sample.

3.6. Application

Modified SiO_2 particles are popular fillers for base oil aimed at improving its tribological properties [52]. In order to estimate antifrictional properties, six compositions were prepared by stirring at room temperature. These are stable suspensions and consist of base oil and the **SiO_2-B_O** or the **SiO_2-B_S** additives (5, 10 and 15 wt.%). Table 2 presents friction coefficients of the base oil and of the base oil with fillers.

The friction coefficients of all studied oils with additives tend to decrease. The most positive effect is obtained for the oil with 5 wt.% of **SiO_2-B_O** and **SiO_2-B_S** for the whole range of applied loads. At 10, 20, 30 and 60 N the friction coefficient is reduced at 3.8, 1.9, 1.5 and 1.1 times, respectively, for **SiO_2-B_O**. And at 10, 20, 30 and 60 N the friction coefficient is reduced 9.9, 1.7, 1.7 and 1.1 times, respectively, for **SiO_2-B_S**. Friction is the least reduced for the oil with 10 wt.% of fillers. The oil with 15 wt.% of the **SiO_2-B_O** and the **SiO_2-B_S** additives takes an intermediate position.

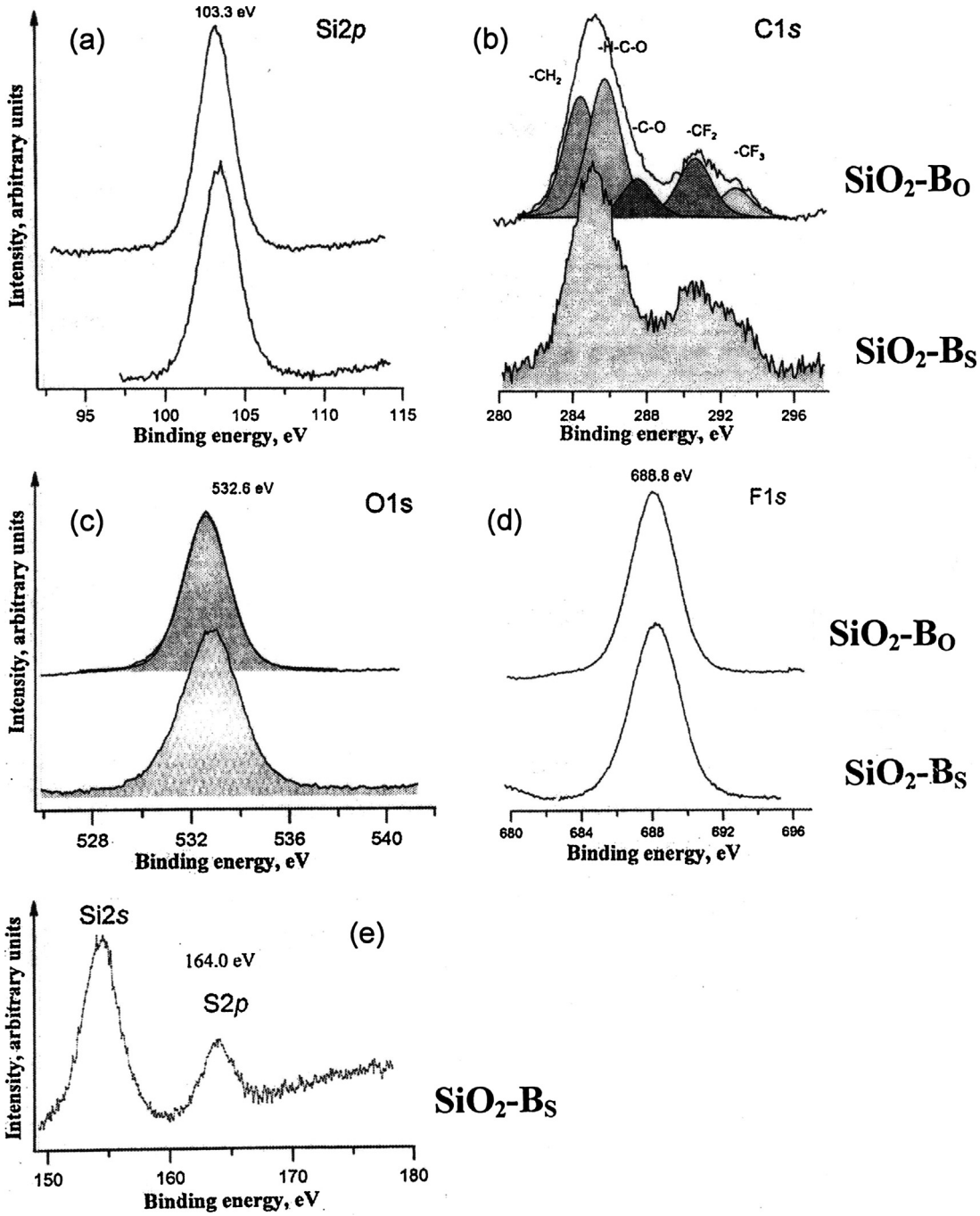

Fig. 4. Representative XPS spectra of hybrid **SiO_2-B_O** and **SiO_2-B_S**: for Si 2p (a), for C 1s (b), O 1s (c), for F 1s (d) and for S 2p (e).

Table 2
Friction coefficients of the base oil and of the base oil with the **SiO_2-B_O** or the **SiO_2-B_S** additives.

Composition contents	Friction coefficients			
	10 N	20 N	30 N	60 N
Base oil (100%)	0.099	0.101	0.107	0.116
Base oil (95%) and SiO_2-B_O (5%)	0.026	0.054	0.071	0.102
Base oil (90%) and SiO_2-B_O (10%)	0.086	0.106	0.092	0.109
Base oil (85%) and SiO_2-B_O (15%)	0.033	0.082	0.092	0.108
Base oil (95%) and SiO_2-B_S (5%)	0.010	0.059	0.063	0.102
Base oil (90%) and SiO_2-B_S (10%)	0.042	0.099	0.092	0.104
Base oil (85%) and SiO_2-B_S (15%)	0.027	0.079	0.083	0.098

The most likely reason for the observed reduced friction in the presence of the **SiO_2-B_O** and the **SiO_2-B_S** fillers is the formation of a lubrication layer at tribochemical reaction. Possibly these boundary films represent iron fluorides as was shown in Ref. [53] where the octadecylamine salt of decapentylfluorooctanic acid was used as an additive. In the case of the **SiO_2-B_S** filler the formation of sulfur-containing iron salts (sulfides, sulfates etc.) is also possible [54,55].

An increase of the **SiO_2-B_O** and the **SiO_2-B_S** concentrations in the oil leads to the appearance of a higher quantity of non-spherical SiO_2 particles in the friction zone. Thus, the SiO_2 particles act as an abrasive, and the surface is rubbed additionally thus losing the boundary lubrication layer, especially for higher loads.

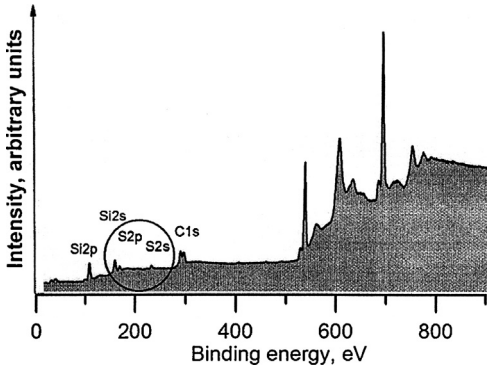

Fig. 5. Binding energy spectrum of the **SiO_2-B_S** sample.

4. Conclusion

In our study a method was proposed of surface modification of SiO_2 particles in sol–gel process at TEOS hydrolysis in the presence of the [(perfluorobutyl)methyl]oxirane and the [(perfluorobutyl)methyl]thiirane at NEt_3 catalysis. The modified SiO_2 particles used as additives to the base oil improve boundary friction. The most reduced friction was observed for the composition with 5 wt.% of the modified SiO_2 particles. The composition can be used for an effective operation of easy and middle load centers equipment.

Acknowledgment

This work is supported by Russian Foundation for Basic Research (Grant no. 13-03-00306).

References

[1] E.O. Oh, R.K. Gupta, C.M. Whang, Effects of pH and dye concentration on the optical and structural properties of coumarin-4 dye-doped SiO_2-PDMS xerogels, J. Sol–Gel Sci. Technol. 28 (2003) 279–288.
[2] V.S. Tripathi, V.B. Kandimalla, H. Ju, Preparation of ormosil and its applications in the immobilizing biomolecules, Sens. Actuators B 114 (2006) 1071–1082.
[3] P. Etienne, J. Denape, J.Y. Paris, J. Phalippou, R. Sempere, Tribological properties of ormosil coatings, J. Sol–Gel Sci. Technol. 6 (1996) 287–297.
[4] R.G. Hu, S. Zhang, J.F. Bu, C.J. Lin, G.L. Song, Recent progress in corrosion protection of magnesium alloys by organic coatings, Prog. Org. Coat. 73 (2012) 129–141.
[5] H.J. Zhou, M.Z. Rong, M.Q. Zhang, B. Lehmann, K. Friedrich, Grafting of poly(glycidyl methacrylate) onto nano-SiO_2 and its reactivity in polymers, Polym. J. 37 (2005) 677–685.
[6] N. Tsubokawa, Surface grafting of polymers onto nanoparticles in a solvent-free dry-system and applications of polymer-grafted nanoparticles as novel functional hybrid materials, Polym. J. 39 (2007) 983–1000.
[7] Y. Yu, M.Z. Rong, M.Q. Zhang, Grafting of hyperbranched aromatic polyamide onto silica nanoparticles, Polymer 51 (2010) 492–499.
[8] J. Livage, C. Sanchez, Sol–gel chemistry, J. Non-Cryst. Solids 145 (1992) 11–19.
[9] V. Cirkva, O. Paleta, B. Ameduri, B. Boutevin, Chemistry of [(perfluoroalkyl)methyl]oxiranes. Regioselectivity of ring opening with O-nucleophiles and the preparation of amphiphilic monomers, J. Fluor. Chem. 84 (1997) 53–61.
[10] A.V. Fokin, A.F. Kolomiets, The reactivity of epithio-compounds, Russ. Chem. Rev. 45 (1976) 25–42.
[11] V. Cirkva, B. Ameduri, B. Boutevin, O. Paleta, Highly selective synthesis of [(perfluoroalkyl)methyl]oxiranes (by the addition of iodoperfluoroalkanes to allyl acetate), J. Fluor. Chem. 83 (1997) 151–158.
[12] J. Costa, M.R. Gallas, E.V. Benvenutti, J.A.H. Da Jornada, Infrared and thermogravimetric study of high pressure consolidation in alkoxide silica gel powders, J. Non-Cryst. Solids 220 (1997) 195–201.
[13] C.E. Fisher, J. Mink, L. Hajba, Z. Bacsik, C. Németh, J. Mihály, A. Raith, M. Cokoja, F.E. Kühn, Vibrational spectroscopic study of SiO_2-based nanotubes, Vib. Spectrosc. 66 (2013) 104–118.
[14] M. Ramezania, M.R. Vaezia, A. Kazemzadeh, Preparation of silane-functionalized silica films via two-step dipcoating sol–gel and evaluation of their superhydrophobic properties, Appl. Surf. Sci. 317 (2014) 147–153.
[15] X. Li, X. Yin, L. Zhang, S. He, The devitrification kinetics of silica powder heat-treated in different conditions, J. Non-Cryst. Solids 354 (2008) 3254–3259.
[16] T.B. Ghosh, K.C. Nandi, H.N. Acharya, D. Mukherjee, X-ray photoelectron spectroscopic analysis of amorphous silica – a comparative study, Mater. Lett. 12 (1991) 175–178.
[17] V.N. Khabashesku, Covalent functionalization of carbon nanotubes: synthesis, properties and applications of fluorinated derivatives, Russ. Chem. Rev. 80 (2011) 705–725.
[18] B. Wang, J. Li, J. Zhang, H. Li, P. Chen, Q. Gu, Z. Wang, Thermo-mechanical properties of the composite made of poly(3-hydroxybutyrate-co-3-hydroxyvalerate) and acetylated chitin nanocrystals, Carbohydr. Polym. 95 (2013) 100–106.
[19] E. Pacard, M.A. Brook, A.M. Ragheb, C. Pichot, C. Chaix, Elaboration of silica colloid/polymer hybrid support for oligonucleotide synthesis, Colloids Surf. B 47 (2006) 176–188.
[20] F. Bucatariu, F. Simon, C. Bellmann, G. Fundueanu, E.S. Dragan, Stability under flow conditions of trypsin immobilized onto poly(vinyl amine) functionalized silica microparticles, Colloids Surf. A 399 (2012) 71–77.
[21] F.J.R. Nieto, E. Fachini, C.R. Cabrera, A.J. Arvia, X-ray photoelectron spectroscopy of oxygen-containing layers formed by a linear potential scan on stepped gold (1 1 1) films in aqueous 1 M sulphuric acid, Thin Solid Films 517 (2009) 1534–1540.
[22] J. Lin, H. Chen, T. fei, J. Zhang, Highly transparent superhydrophobic organic–inorganic nanocoating from the aggregation of silica nanoparticles, Colloids Surf. A 421 (2013) 51–62.
[23] L. Wang, Y. Tian, H. Ding, J. Li, Microstructure and properties of organosoluble polyimide/silica hybrid films, Eur. Polym. J. 42 (2006) 2921–2930.
[24] W. Liao, H. teng, J. Qu, T. Masuda, Fabrication of chemically bonded polyacrylate/silica hybrid films with high silicon contents by the sol–gel method, Prog. Org. Coat. 71 (2011) 376–383.
[25] Y. Zhang, Z. Wang, W. Zhou, G. Min, M. Lang, Cationic poly(ε-caprolactone) surface functionalized mesoporous silica nanoparticles and their application in drug delivery, Appl. Surf. Sci. 276 (2013) 769–775.
[26] S.W. Woo, M.Y. Song, J.S. Rho, Y.S. Lee, The effect of oxyfluorination on the surface characteristics of low-density polyethelene films, J. Ind. Eng. Chem. 11 (2005) 55–61.
[27] L. Raiado-Pereira, A.P. Carapeto, A.M. Botelho do Rego, M. Mateus, Grafting hydrophobic and affinity interaction ligands on membrane adsorbers: a close-up "view" by X-ray photoelectron spectroscopy, Sep. Purif. Technol. 93 (2012) 75–82.
[28] G. Beamson, Conformation effects in the XPS valence band spectra of aliphatic polyesters, J. Electron Spectrosc. 154 (2007) 83–89.
[29] G.P. López, D.G. Gastner, B.D. Ratner, XPS O 1s binding energies for polymers containing hydroxyl, ether, ketone and ester groups, Surf. Interface Anal. 17 (1991) 267–272.
[30] J. Lin, X. Wu, C. Zheng, P. Zhang, B. huang, N. Guo, L. Jin, Synthesis and properties of epoxy-polyurethane/silicananocomposites by a novel sol method and in-situ solutionpolymerization route, Appl. Surf. Sci. 303 (2014) 67–75.
[31] L. Bistričić, G. Baranović, M. Leskovac, E. Govorčin Bajsić, Hydrogen bonding and mechanical properties of thin films of polyether-based polyurethane–silica nanocomposites, Eur. Polym. J. 46 (2010) 1975–1987.
[32] J.S. Lim, I. Noda, S.S. Im, Effect of hydrogen bonding on the crystallization behavior of poly(3-hydroxybutirate-*co*-3-hydroxyhexanoate)/silica hybrid composites, Polymer 48 (2007) 2745–2754.
[33] B. Buszewski, S. Bocian, G. Rychlicki, M. Matyska, J. Pesek, Determination of accessible silanols groups on silica gel surfaces using microcalorimetric measurements, J. Chromatogr. A 1232 (2012) 43–46.
[34] A. Dkhissi, A. Estéve, L. Jeloaica, M. Djafari Rouhani, G. Landa, Substrate size effect in the modeling of molecular grafting: case of organo-silane chains on silica, Chem. Phys. 323 (2006) 179–184.
[35] S. Kawano, A. Sei, M. Kunitake, Thixotropic interparticle interaction between silica and nonionic polymer particles prepared by static dispersion polymerization, Polymer 52 (2011) 1577–1588.
[36] S. Saïdi, F. Guittard, C. Guimon, S. Géribaldi, Synthesis and characterization of copolymers based on styrene and partially fluorinated acrylates, Eur. Polym. J. 42 (2006) 702–710.
[37] X. Xiao, J. Liu, Synthesis and characterization of fluorine-containing polyacrylate emulsion with core–shell structure, Chin. J. Chem. Eng. 16 (2008) 626–630.
[38] H. Xin, Y. Shen, X. Li, Novel cationic polyurethane-fluorinated acrylic hybrid latexes: synthesis, characterization and properties, Colloids Surf. A 384 (2011) 205–211.
[39] Z. Yan, W. Liu, N. Gao, H. Wang, K. Su, Synthesis and properties of a novel UV-cured fluorinated siloxane graft copolymer for improved surface, dielectric and tribological properties of epoxy acrylate coating, Appl. Surf. Sci. 284 (2013) 683–691.
[40] Y. Li, Y. Su, X. Zhao, R. Zhang, J. Zhao, X. Fan, Z. Jiang, Surface fluorination of polyamide nanofiltration membrane for enhanced antifouling property, J. Membr. Sci. 455 (2014) 15–23.
[41] M. Aminuzzaman, M. Mitsuishi, T. Miyashita, Surface modification of a flexible polyimide film using a reactive fluorinated polymer nanosheet, Thin Solid Films 519 (2010) 974–977.
[42] A. Torrisi, XPS study of five fluorinated compounds deposited on calcarenite stone. Part I. Unaged samples, Appl. Surf. Sci. 254 (2008) 2650–2658.
[43] A. Torrisi, XPS study of five fluorinated compounds deposited on calcarenite stone. Part II. Aged samples, Appl. Surf. Sci. 254 (2008) 7127–7136.
[44] W. Tang, Y. Huang, W. Meng, F.-L. Qing, Synthesis of fluorinated hyperbranched polymers capable as highly hydrophobic and oleophobic coating materials, Eur. Polym. J. 46 (2010) 506–518.

[45] A. Qu, X. Wen, P. Pi, J. Cheng, Z. Yang, Gradient distribution of fluorine on the film surface of the organic–inorganic hybrid fluoropolymer, Colloids Surf. A 345 (2009) 18–25.
[46] I. Jerman, B. Orel, A.S. Vuk, M. Koželj, J. Kovač, A structural and corrosion study of triethoxysilyl and perfluorooctyl functionalized polyhedral silsesquioxane nanocomposite films on AA 2024 alloy, Thin Solid Films 518 (2010) 2710–2721.
[47] F. Morel, V. Bounor-Legaré, E. Espuche, O. Persyn, M. Lacroix, Surface modification of calcium carbonate nanofillers by fluoro- and alkyl-alkoxysilane: consequences on the morphology, thermal stability and gas barrier properties of polyvinylidene fluoride nanocomposites, Eur. Polym. J. 48 (2012) 919–929.
[48] N. Dupuy, A. Pasc, F. Baros, C. Gérardin, Langmuir isotherm analysis of novel branched per-fluorinated surfactants and their interactions with single stranded DNA, J. Fluor. Chem. 132 (2011) 892–897.
[49] J.P. Yang, D.X. Yuan, B. Zhou, J. Gao, H.G. Ni, L. Zhang, X.P. Wang, Studies on the effect of the alkyl group on the surface segregation of poly(*n*-alkyl methacrylate) end-capped 2-perfluorooctylethyl methacrylate films, J. Colloid Interface Sci. 359 (2011) 269–278.
[50] G. Chang, L. He, J. Liang, N. Wang, R. Cao, X. Zhao, Polysiloxane/poly(fluorinated acrylate) core–shell latexes and surface wettability of films, J. Fluor. Chem. 158 (2014) 21–28.
[51] T. Schuster, J.W. Krumpfer, S. Schellenberger, R. Friedrich, M. Klapper, K. Müllen, Effect of chemical structure on the dynamic and static surface tensions of short-chain, multi-arm nonionic fluorosurfactants, J. Colloid Interface Sci. 428 (2014) 276–285.
[52] Y. Kang, X. Chen, S. Song, L. Yu, P. Zhang, Friction and wear behavior of nanosilica-filled epoxy resin composite coatings, Appl. Surf. Sci. 258 (2012) 6384–6390.
[53] G. Gu, Z. Wu, Z. Zhang, F. Qing, Tribological properties of fluorine-containing additives of silicone oil, Tribol. Int. 42 (2009) 397–402.
[54] A. Nevile, A. Morina, T. Hague, M. Voong, Compatibility between tribological surfaces and lubricant additives – how friction and wear reduction can be controlled by surface/lube synergies, Tribol. Int. 40 (2007) 1680–1695.
[55] H. Ma, J. Li, H. Chen, G. Zuo, Y. Yu, T. Ren, Y. Zhao, XPS and XANES characteristics of tribofilms and thermal films generated by two P- and/or S-containing additives in water-based lubricant, Tribol. Int. 42 (2009) 940–945.